Site dependence of the local density of unoccupied states - an aid for understanding trends in x-ray absorption fine structure

2001 J. Phys.: Condens. Matter 13 4291

(http://iopscience.iop.org/0953-8984/13/19/309)

INSTITUTE OF PHYSICS PUBLISHING JOURNAL OF PHYSICS: CONDENSED MATTER

J. Phys.: Condens. Matter **13** (2001) 4291–4302 www.iop.org/Journals/cm PII: S0953-8984(01)19286-6

Site dependence of the local density of unoccupied states—an aid for understanding trends in x-ray absorption fine structure

O Šipr

Institute of Physics, Academy of Sciences of the Czech Republic, Cukrovarnická 10, 162 53 Praha 6, Czech Republic

E-mail: sipr@fzu.cz

Received 22 November 2000, in final form 20 March 2001

Abstract

The site dependence and degree of localization of the total density of unoccupied states around various atoms inside a finite cluster are investigated, with the aim of exploring the potential of this kind of analysis for understanding some trends in calculated x-ray absorption near-edge-structure (XANES) spectra. The local density of states (DOS) around atoms at the surface of a cluster is in principle quite similar to the DOS around atoms in its interior; the only difference is that the heights of the peaks in the DOS are much smaller around the surface atoms than around the bulk ones. The proximity of a surface has a lesser effect on the DOS around subsurface atoms than the presence of a large number of other atoms in the bulk region of a large cluster. The fine structure in the excess density of states, evaluated via the Lloyd formula, is almost exclusively generated inside the cluster under study. Analysing the local DOS increases our understanding of distinct peculiarities in the cluster-size effect in XANES spectra in some cases.

1. Introduction

X-ray absorption fine-structure (XAFS) analysis has become a widely used tool for investigating both structural and electronic properties of solids. There has been significant progress in theoretical modelling of XAFS (see, e.g., the recent review [1]), which enhances our ability to extract useful information from experiment. Far above the edge, i.e., for photoelectron energies of more than $\sim$100 eV, the underlying physics can be well understood in terms of single backscatterings of the excited electron from neighbouring atoms. On the other hand, in the near-edge region, a gap still persists in our ability to *intuitively understand* and interpret the data—even in cases where the theory reproduces the experiment fairly accurately. Having a more illustrative representation of that process which gives rise to the observed fine structure would, among other things, improve our ability to employ x-ray absorption near-edge-structure (XANES) spectroscopy for studying the structure of non-crystalline materials.

0953-8984/01/194291+12$30.00

There are several ways to calculate XANES spectra. The most universal one seems to be the real-space multiple-scattering method [2]. In this method, an infinite bulk solid is replaced by a finite cluster of ∼50–150 atoms, and the fine structure is generated by mutual interference between all possible multiple-scattering paths connecting the atoms of the respective cluster. Scattering amplitudes and scattering matrices are thus key concepts in this formalism. These concepts proved to be quite useful also in interpreting some trends and features in XAFS—let us recall, e.g., the so-called 'focusing effect' which explains why a multiple-scattering signal even from distant shells is sometimes quite important for generating an XAFS signal, to mention just one example [3]. In this paper, however, we want to concentrate on a different notion, namely, on the density of states.

Density of states (DOS) can be viewed as a complementary concept to the scattering terminology: the local density of states can be expressed via the Green function of the electron $G(\boldsymbol{r}, \boldsymbol{r}; E)$ as

$$n(\boldsymbol{r}, E) = -\frac{2}{\pi} \operatorname{Im} G(\boldsymbol{r}, \boldsymbol{r}; E) \tag{1}$$

and there is a one-to-one correspondence between the Green function operator $G(E)$ and the scattering T-matrix operator $T(E)$ (see, e.g., equations (48) of [4] or the reviews [2, 5]). Indeed, an x-ray absorption spectrum can be viewed as an appropriate angular-momentum-projected component of the DOS around the photoabsorbing atom, weighted by a transition matrix element [6, 7]. This line of research has been pursued mostly in connection with band-structure calculations.

In this paper, the emphasis is laid on another aspect of the local DOS, namely, on its site dependence. For a finite cluster, spatial variations in the local density of unoccupied states $n(\boldsymbol{r}, E)$, when moving the radius vector $\boldsymbol{r}$ from the neighbourhood of one atom to another, reflect different probabilities for an excited electron to be found in the vicinity of the respective atom. Note that the probability reflected by $n(\boldsymbol{r}, E)$ is 'isotropic', in the sense that it does not take into account the fact that the photoelectron, which generates the XAFS signal, is ejected from a particular atom located at $\boldsymbol{R}^{(0)}$, with a specific angular momentum with respect to $\boldsymbol{R}^{(0)}$. One would have to turn to a different concept, namely the *probability density of the excited photoelectron* [8], in order to employ that additional characteristic as well.

The local density of states $n(\boldsymbol{r}, E)$, explored in this paper, provides thus only limited information about the localization of the real XAFS photoelectron. On the other hand, the local DOS is a well-defined and well-understood quantity and can be relatively easily evaluated using commonly used XANES codes (such as ICXANES [9], CONTINUUM [10] or FEFF [11]), even around atoms which are not in the centre of the test cluster. Therefore, it is worth exploring its potential for explaining at least some aspects of XANES spectra. Such a study could have wider implications as well, as cluster models are often employed for investigations of the electronic structure of solids in general.

The main purpose of this paper is to help in understanding the importance of individual atoms for generating XANES peaks by exploring the total DOS in the vicinity of those atoms and by comparing it with the DOS around other atoms of the same cluster. Additionally, a better insight into the physics of XANES formation is sought by studying the site dependence of the DOS in a chemically uniform finite cluster and the degree of localization of the unoccupied electron states in a cluster in general. We begin by investigating the spatial dependence and degree of localization of the unoccupied DOS around atoms in test clusters. Then we will turn to inspecting to what extent DOS analysis can be helpful in understanding particular problems in XANES interpretation.

2. Spatial variation of the local DOS

In this section, the cluster-size convergence of the local DOS calculation will be investigated. We will concentrate on a large cluster of atoms of identical chemical type, and examine how the local density of unoccupied states varies across the cluster. The aim is to find out how the calculated DOS around particular atoms in a test cluster (and, presumably, also the scattering property) is influenced by the proximity of the cluster surface.

We calculate the site-dependent total DOS per unit volume inside a Wigner–Seitz sphere around the jth atom at position $\boldsymbol{R}^{(j)}$, relying on the relation [2,5]

$$n_{\mathrm{clu}}^{(j)}(E) = -\frac{1}{V^{(j)}} \oint_{V^{(j)}} \mathrm{d}\boldsymbol{r}\, \frac{2}{\pi} \operatorname{Im} G(\boldsymbol{r}-\boldsymbol{R}^{(j)}, \boldsymbol{r}-\boldsymbol{R}^{(j)}; E) = -\frac{1}{k} \sum_{L}^{L_{\max}} F_{\ell}^{(j)} \operatorname{Im} \tau_{LL}^{jj} \tag{2}$$

assuming the muffin-tin approximation. The angular-momentum subscript L stands for the pair (ℓ, m) and $V^{(j)}$ is the volume of the Wigner–Seitz sphere (or any other suitably chosen normalization sphere). The atomic factor is

$$F_{\ell}^{(j)} = \frac{1}{V^{(j)}} \int_0^{R_{WS}} \mathrm{d}r\, r^2 \, [\mathcal{R}_{\ell}(r)]^2 \tag{3}$$

and the radial solution of a single-site Schrödinger equation $\mathcal{R}_{\ell}(r)$ is normalized so that its asymptotic form is

$$\mathcal{R}_{\ell}(r) \approx \sqrt{\frac{2}{\pi}} k \, [\, j_{\ell}(kr) \operatorname{cotan} \delta_{\ell} - n_{\ell}(kr)] \, . \tag{4}$$

The matrix $\tau_{LL'}^{ij}$, entering equation (2) through its diagonal elements, is basically a scattering-path operator [12], defined here as in equation (2.4) of [13] or equation (2.4) of [9]. To make contact with other works, let us just note that this τ-matrix is related, e.g., to the $(\underline{T} + \underline{H})$-matrix of [14] via

$$\tau_{LL'}^{ij} = -\left[(\underline{T} + \underline{H})^{-1} \right]_{L'L}^{ji} . \tag{5}$$

All of the equations presented above are in Rydberg atomic units.

Let us concentrate on bulk crystalline copper as an illustrative example—a material frequently employed in various test studies. All of the calculations presented here were performed using the RSMS code [15], which is essentially an amended and upgraded ICXANES program [9]. We considered a cluster of 555 atoms, including thereby 19 coordination spheres, the most distant of them being at a distance of 11.42 Å (21.57 au) from the central atom. The radius of the normalization sphere R_{WS} is 1.41 Å (2.67 au). In evaluating the τ-matrix, the division of the whole cluster into concentric shells was employed; thus the intershell and intrashell scattering were calculated separately [13]. The maximum angular momentum included in the single-site scattering was $\ell_{\max} = 4$; the maximum angular momentum included in the intershell scattering was $\ell_{\mathrm{out}} = 12$. We checked both of these limits for convergency. The self-consistent muffin-tin potential of Moruzzi *et al* [16] was used for all atomic sites, meaning that atoms at the periphery of the cluster have the same potential as those inside it. That would be inadequate if we were concerned with real clusters; however, the clusters that we are interested in simulate a bulk solid, and so taking atomic potentials independent of the position in the cluster is a reasonable prescription.

The dependence of the local DOS on the position of the atom is investigated in a twofold way. First, we consider the above-mentioned fixed cluster of 555 atoms and calculate the DOS around each of its atoms (figure 1(a)). In order to isolate the net effect of the cluster, we

subtract the DOS around a single muffin-tin sphere (one-atom cluster), $n_{\mathrm{at}}^{(j)}(E)$, from the DOS around the jth atom in a large cluster, $n_{\mathrm{clu}}^{(j)}(E)$:

$$n_{\mathrm{diff}}^{(j)}(E) \equiv n_{\mathrm{clu}}^{(j)}(E) - n_{\mathrm{at}}^{(j)}(E). \tag{6}$$

In this way, the influence of the single-site atomic-like potential is filtered out from our data. Our $n_{\mathrm{diff}}^{(j)}$ results are shown in figure 2(a) (left panel). Second, these curves are to be compared with the local DOS around atoms at the centres of smaller clusters chosen such that they represent the 'symmetric parts' of the surroundings of respective atoms in the larger cluster (figure 1(b)). These results are displayed in figure 2(b) (right panel). The curves in the left and right panels of figure 2 thus correspond pairwise to each other: the atom around which the local DOS is investigated is the same for both curves of the pair—only different kinds of surroundings are considered in each of the cases (a non-centrosymmetric cluster of 555 atoms in the left panel, and its smaller, centrosymmetric subsection in the right panel). Note that atoms located in the 13th sphere and beyond are already so close to the surface that no other atoms occur within the surface-touching spheres circumscribed around them (cf. the three uppermost 'curves' in the left panel of figure 2, which represent thus the pure single-site DOS).

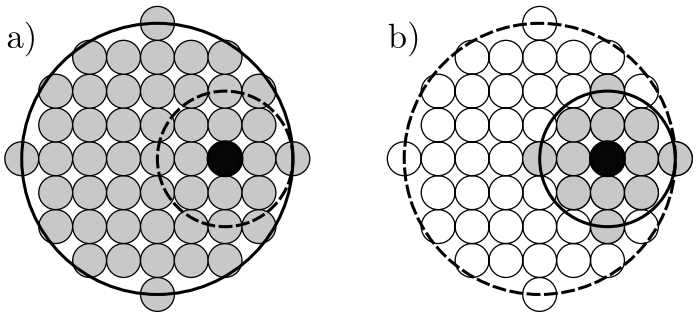

Figure 1. Two kinds of surroundings of a particular atom in a large cluster. First, the atom is surrounded by all other atoms in the cluster ((a), left diagram). Second, only those atoms which fall inside a sphere inscribed around the atom investigated so that it touches the surface of the original cluster are considered ((b), right diagram). The atom investigated is shown as a black circle; atoms which are taken into account are represented by grey circles.

By inspecting figure 2(a), we can observe that a bulk-like behaviour switches gradually to a surface-like one for atoms lying somewhere between the 7th and 13th coordination spheres of the 555-atom cluster. Note that although the DOS around atoms close to the cluster surface differs only slightly from the atomic DOS (uppermost curves in 2(a)), even that slight deviation retains its bulk-like features—the curves are just strongly smeared and decreased in their amplitude. No new features appear in the DOS when moving from the centre towards the surface—all that happens is that the bulk-like peaks get more and more blurred when the surface is being approached. It seems, therefore, that for a particular atom, the mere presence of its neighbours at given distances is more important than the overall geometry of its surroundings. This 'no new feature' property of the DOS at surface atoms has its analogue in XANES as well [17].

Comparing figure 2(a) with figure 2(b), it is evident that the 'bulk' character of the local DOS is significantly determined by the non-symmetric, protruding part of the surroundings of the respective atom (cf. parts (a) and (b) of figure 1): for atoms buried as deeply as those in the fifth shell, there is already a distinct difference between the DOS calculated by taking

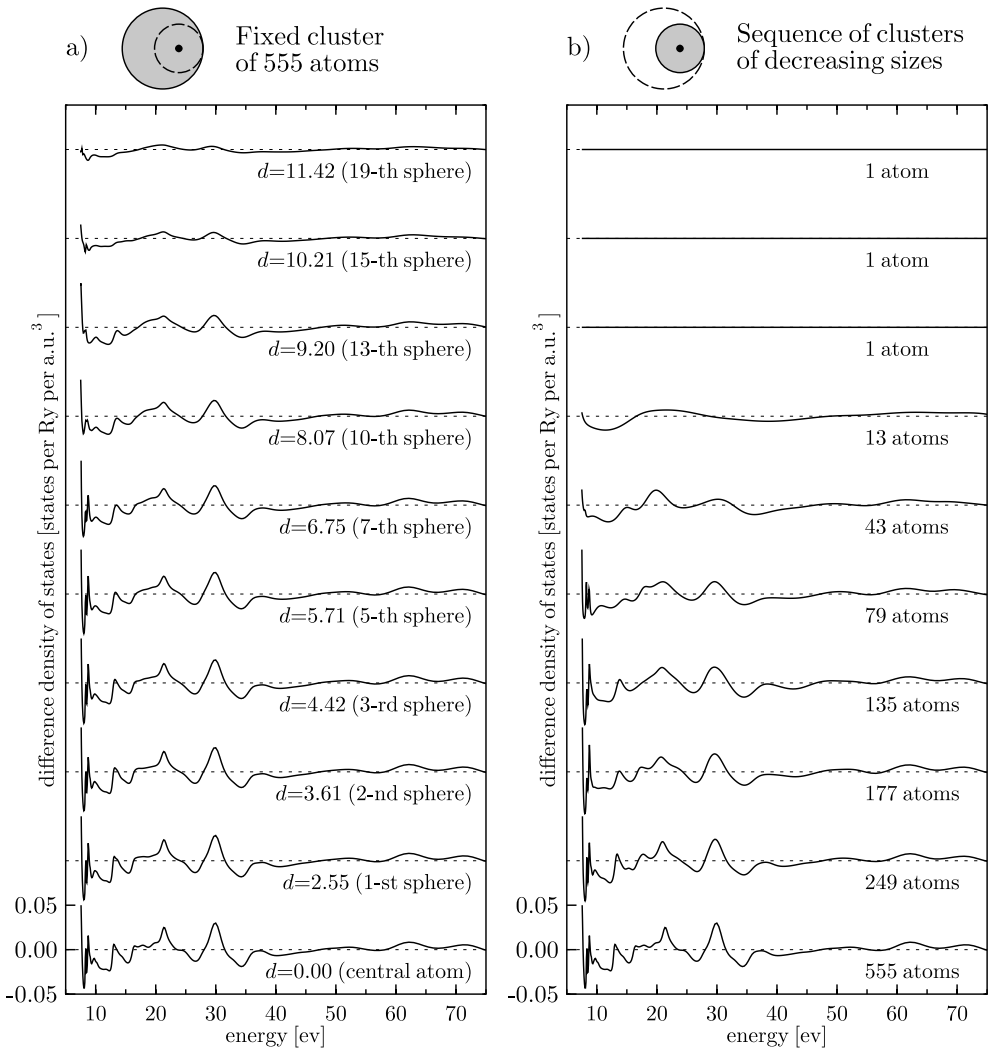

Figure 2. The site-dependent difference density of states $n^{(j)}_{\mathrm{diff}}(E)$ around atoms in a large 555-atom cluster of copper, calculated by including the whole surroundings of each atom ((a), left panel) and by taking into account only its centrosymmetric part ((b), right panel). Each curve in the left panel is identified by the order of the coordination sphere to which the atom investigated belongs (its distance d from the centre in Å is also shown). Corresponding curves in the right panel are labelled with the sizes of appropriate centrosymmetric clusters. The zero of energy coincides with the muffin-tin zero.

into account the whole cluster of 555 atoms and that calculated by taking into account only its 'symmetric' subsection (containing 79 atoms in this case). In other words, for a large cluster, the very fact that a surface occurs somewhere near a particular atom is to a large extent compensated by the presence of a large number of even quite distant atoms in the rest of the cluster. Hence, when applying the cluster method [9–11] for calculating the XANES of multicomponent materials, one can be confident that the 'surface effect' of the model cluster dies out quite quickly with distance of atoms from the surface, and the differences between chemical species would thus prevail.

3. Localization of excess DOS

Let us turn now to the problem of localization of unoccupied electron states inside a cluster. The famous Lloyd formula tells us what the difference is between the overall number of electrons with energies less than E in the case where there is a cluster of atoms in the space and that in the case where the space is empty [4]. We present it here in a computer-code-oriented form:

$$\Delta N(E) \equiv N(E) - N_0(E) = \frac{2}{\pi} \,\mathrm{Im}\, \ln \det \left[\delta_{LL'} + T^{\mathrm{IO}}_{LL'}\right] \tag{7}$$

where $T^{\mathrm{IO}}_{LL'}$ is the in–out scattering matrix defined via equation (2.7) of [13]. Equation (7) can be directly obtained from equation (29) of [4] by employing equations (98) and (142) of [4] and comparing the definitions for free-electron propagators in [4] and in [13]. Note that the quantity $\Delta N(E)$ is dimensionless. By differentiating it with respect to energy, we get the excess density of states, $\Delta n_{\mathrm{tot}}(E)$, which describes how the presence of the cluster affects the 'originally' free-electron DOS:

$$\Delta n_{\mathrm{tot}}(E) \equiv \frac{\mathrm{d}[\Delta N(E)]}{\mathrm{d}E}. \tag{8}$$

There is yet another way of calculating the excess density of states, namely, by taking the density of states $n^{(j)}_{\mathrm{clu}}(E)$ evaluated from equation (2) and subtracting from it the free-electron density of states $n^{(j)}_0(E)$ around every atom inside the cluster:

$$\Delta n_{\mathrm{loc}}(E) = \sum_j V^{(j)}[n^{(j)}_{\mathrm{clu}}(E) - n^{(j)}_0(E)]. \tag{9}$$

The excess DOS evaluated in this way incorporates, however, only that portion of the space which is occupied by atoms of the respective cluster—contrary to $\Delta n_{\mathrm{tot}}(E)$ evaluated from equations (7) and (8), which includes the excess DOS produced in the outer space as well. Thus by comparing $\Delta n_{\mathrm{tot}}(E)$ with $\Delta n_{\mathrm{loc}}(E)$, we can learn to what degree the influence of the cluster on the unoccupied DOS is *spatially confined* to the cluster itself, and to what degree it 'spills over'.

For a test material, we turn again to bulk copper (as in section 2). We calculated the total excess DOS $\Delta n_{\mathrm{tot}}(E)$ via (7) and (8), the local excess DOS $\Delta n_{\mathrm{loc}}(E)$ via (9) and the 'outer' excess DOS $\Delta n_{\mathrm{out}}(E)$ defined as their difference:

$$\Delta n_{\mathrm{out}}(E) \equiv \Delta n_{\mathrm{tot}}(E) - \Delta n_{\mathrm{loc}}(E) \tag{10}$$

for various cluster sizes. Note that for the sake of numerical consistency, the free-electron DOS $n^{(j)}_0(E)$ entering equation (9) ought to be evaluated using formally the same equations and procedures as for $n^{(j)}_{\mathrm{clu}}(E)$, replacing just the radial wave function $\mathcal{R}_\ell(r)$ of (4) with $(2/\pi)kj_\ell(kr)$. Finally, we divide all three kinds of excess DOS by the number of atoms in each cluster, in order to filter out the 'extensive' effect of the cluster size.

The results are shown in figure 3 for a few representative cluster sizes. As in section 2, all atoms were attributed the same potential [16], regardless of their location in the cluster. In order to get reliable numbers, the matrix $T^{\mathrm{IO}}_{LL'}$ entering the Lloyd formula (7) has to be quite large—we included angular-momentum components up to $\ell_{\mathrm{inc}} = 36$, though more-or-less convergent curves were obtained already for $\ell_{\mathrm{inc}} > 25$ (especially for smaller clusters). The differentiation in equation (8) was done numerically. We display here only the $E \geqslant 10$ eV region, as wild oscillations make a reliable evaluation of equations (7) and (8) extremely demanding and it is, anyway, only the region above the Fermi level (8.5 eV for the potential of [16]) which is relevant for unoccupied states.

By inspecting figure 3, we can see that almost all of the fine structure in the excess DOS is of local origin. This is understandable, as the fine structure may arise only due to multiple

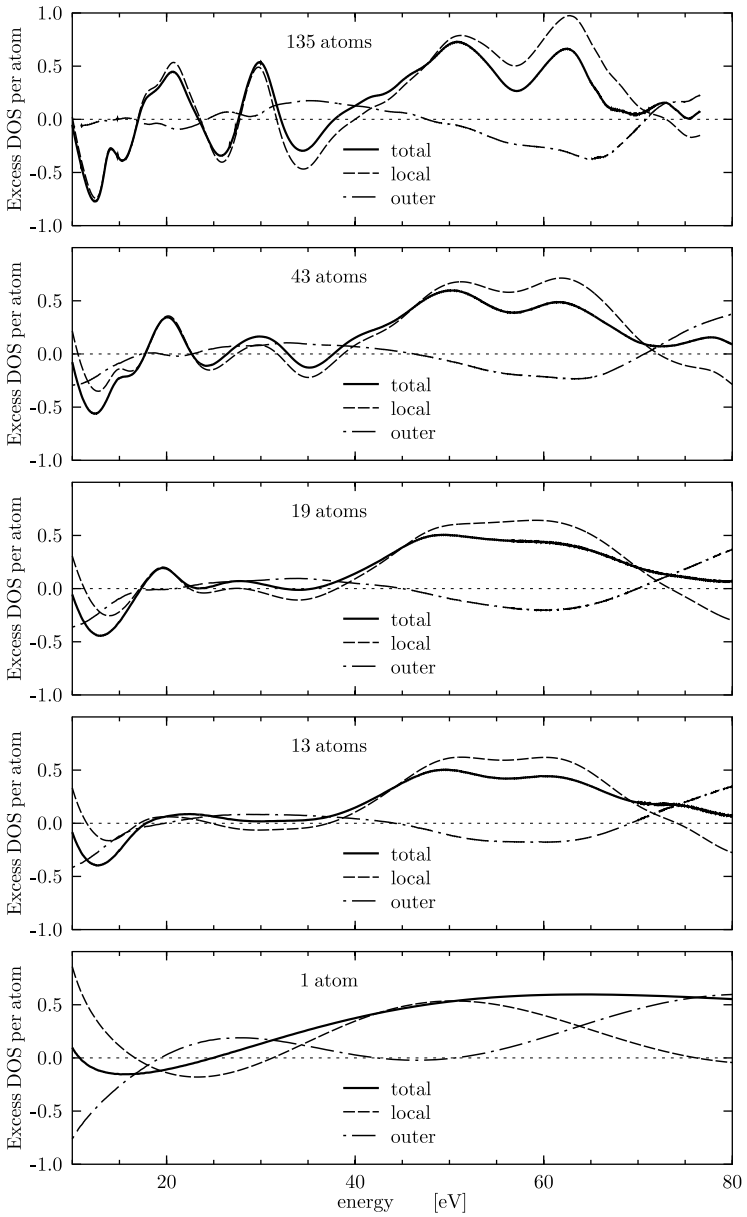

Figure 3. Excess densities of states of electrons in copper clusters of varying sizes. The total excess DOS per atom $\Delta n_{\mathrm{tot}}(E)$ is shown by solid lines, its local component $\Delta n_{\mathrm{loc}}(E)$ by broken lines and the outer part $\Delta n_{\mathrm{out}}(E)$ is represented by chain lines. Sizes of respective clusters are indicated in the plots. The vertical axis is in states per rydberg.

scattering within the cluster. Maybe more surprisingly, there is only a mild dependence of the excess DOS per atom on the size of the cluster. In fact, the largest change occurs between the single-atom case and the 13-atom cluster (the two lowermost panels of figure 3). Nearly all of the fine structure which can be observed in the 135-atom curve is already present for a 43-atom cluster.

The overall ratio between the local ($\Delta n_{\rm loc}(E)$) and the outer ($\Delta n_{\rm out}(E)$) components of the excess DOS does not depend on the size of the cluster involved. The outer excess DOS has nearly the same character for all cluster sizes and exhibits only a weak fine structure. This can be regarded as a sign that the outer space—beyond the proper cluster region—is in fact not very important for unoccupied electron states. This helps one to understand the success of the cluster approach to calculating XANES of bulk solids: the significant physics is already contained in the interior of the cluster.

4. Interplay between local DOS and XANES features

As stated in the introduction, we aim at elucidating some features of XANES by analysing the local site-dependent DOS around atoms constituting the cluster involved in the calculation. We concentrate on one specific issue—cluster-size convergence of the calculated spectra. We choose the XANES of ZnS and of $TiTe_2$ for illustration, as in those cases interesting trends were observed in previous studies [18, 19].

4.1. XANES spectra of ZnS

Coordination spheres around Zn and S atoms in ZnS are formed by atoms of alternating chemical types. XANES spectra of ZnS at both Zn and S K edges were studied comprehensively by Sainctavit *et al* [18, 20]. By investigating the effect of the size of the cluster on XANES spectra, they found an important difference between the role played by coordination spheres made of zinc and sulphur atoms: adding a sphere of Zn atoms to the cluster did not change the resulting spectrum significantly, while adding a sphere of S atoms had a marked influence on the spectrum [18]. Sainctavit *et al* suggested a small scattering amplitude of Zn atoms as the cause for this behaviour. They also observed that a cluster comprising five coordination spheres (47 atoms) is needed to reproduce the Zn spectrum, in contrast to as many as eight coordination spheres (99 atoms) being required for the S-edge reproduction. This was attributed to the focusing effect between the second and the eighth coordination spheres, which gets revealed only if these shells are occupied by strongly scattering sulphur atoms, i.e., at the S edge only [20].

In order to see how these properties translate into the site-dependent DOS language, we considered a single large Zn-centred cluster of 525 atoms and evaluated the local DOS per unit volume around all its atoms. Similarly to in [18, 20], we employed a non-self-consistent potential constructed via a Mattheiss prescription (see, e.g., [21] for a detailed description of the way in which the potential was constructed). The normalization radii R_{WS} were set to 1.13 Å (2.16 au) for both Zn and S spheres, coinciding with the muffin-tin radius of Zn atoms (the sulphur muffin-tin radius was 1.18 Å). All other 'technical' parameters are the same as in section 2. The results are summarized in figure 4. As in the case of bulk copper, we plot in fact the differences $n^{(j)}_{\rm diff}(E)$ between the DOS around atoms in a ZnS cluster and the DOS of isolated atoms of the appropriate chemical type (cf. equation (6)). The atomic-like DOS around isolated Zn and S atoms is shown in the lower panels of figure 4.

The first interesting thing to observe is that, when approaching the periphery of the cluster, the local DOS around Zn atoms relaxes to its atomic-like form much more quickly than that around S atoms. In fact, even for the outermost shell, the DOS around S atoms still does not reduce to its single-atom form. This is in contrast both with the case for Zn atoms in the same cluster and, also, that with Cu atoms in copper (cf. figure 2). This peculiarity of sulphur may

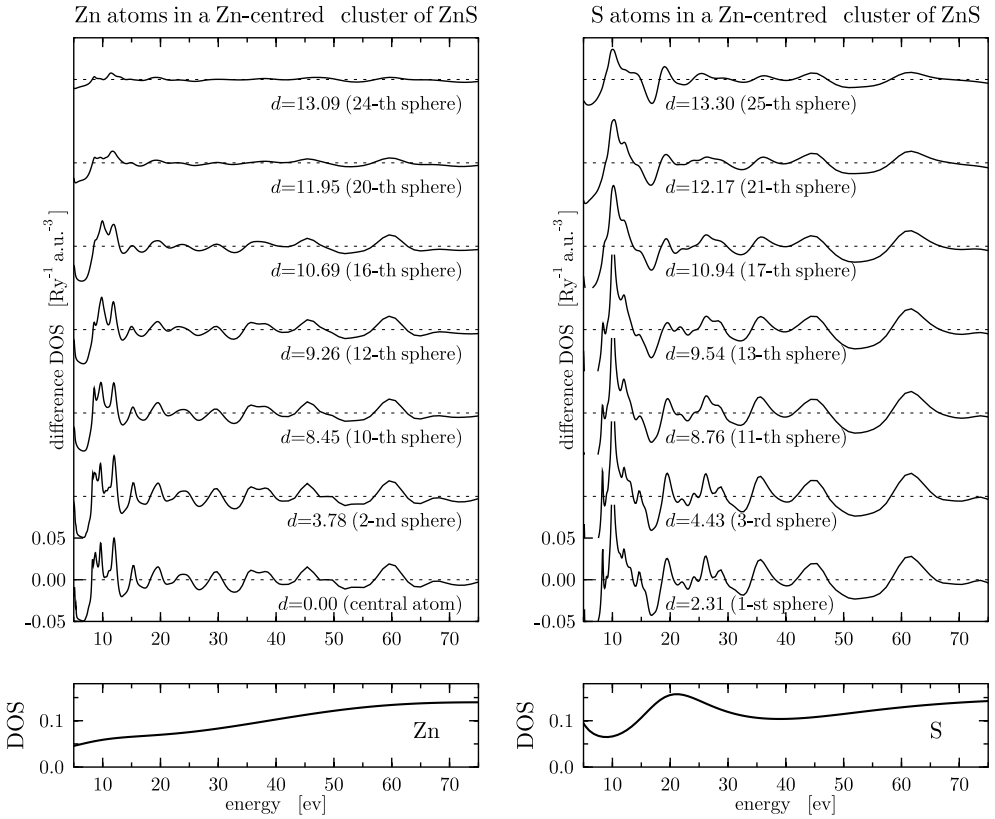

Figure 4. The site-dependent difference density of states $n^{(j)}_{\mathrm{diff}}(E)$ around Zn atoms (left panel) and S atoms (right panel) in a Zn-centred cluster of 525 atoms of ZnS. Each curve is identified by the order of the corresponding coordination sphere around the central Zn atom and by its distance from it in Å. The two lower panels display the total DOS around isolated Zn and S atoms $n^{(j)}_{\mathrm{at}}(E)$. The units on the vertical axes are in states per Ryd per au^3 in all panels.

be a consequence of the fact that its lowest atomic unoccupied states are located closer to the nucleus than the highly delocalized lowest unoccupied states of atomic Cu or Zn. Thus, in a crystal, these states are more sensitive to minor changes of the *local* surroundings of a sulphur atom than in the case of Cu or Zn. However, no definitive conclusions regarding this peculiar property of S atoms can be made without further research.

The two lowermost panels of figure 4 reveal that the DOS around sulphur atoms is indeed larger than that around Zn atoms, especially within the first 30 eV above the muffin-tin zero, which is the range probed by studies of Sainctavit *et al* [18,20]. Hence, from the site-dependent DOS point of view also, it is only natural that inclusion of sulphur spheres has a much more dramatic effect on calculated XANES spectra than inclusion of zinc spheres.

There is no big difference between the local DOS around S atoms belonging to different coordination spheres. Therefore, the significance of the eighth coordination sphere for the S-edge XANES spectrum, observed in [20], cannot be caused by pure DOS-like effects—rather, it has to be a consequence of a complex interference pattern of electron waves, in accordance with the interpretation suggested by Sainctavit *et al*.

Thus, in this case, the DOS-oriented analysis supports and further elucidates the intuitive understanding based on the scattering terminology.

4.2. XANES spectra of $TiTe_2$

$TiTe_2$ is a layered material of the dichalcogenide family. Both Ti K-edge and Te L_1-edge XANES spectra display distinct polarization dependence [19, 22]. Similarly to in the case of ZnS, the convergence of the calculated spectra with respect to the size of the cluster is different for the Ti and the Te edges: it was found that at least 51 atoms are needed to get a converged Ti-edge spectrum (a cluster of 25 atoms is insufficient), while 105 atoms are needed to get a converged Te-edge spectrum (57 atoms are far too few) [19].

In order to get insight into the problem, we calculated the site-dependent total DOS around each of the atoms of a Ti-centred cluster of $TiTe_2$, containing 135 atoms altogether. Due to the poor intershell scattering convergence (in $\ell_{\rm out}$), the whole cluster was treated as a single shell with maximum single-site angular momentum $\ell_{\rm max} = 3$. The muffin-tin potential according to the Mattheiss prescription was generated with muffin-tin radii of 1.37 Å (2.59 au) for Ti and 1.31 Å (2.47 au) for Te atoms. The normalization radius R_{WS} was identical to the Te muffin-tin radius. The results are summarized in figure 5. Analogously to figure 4, the atomic-like DOS

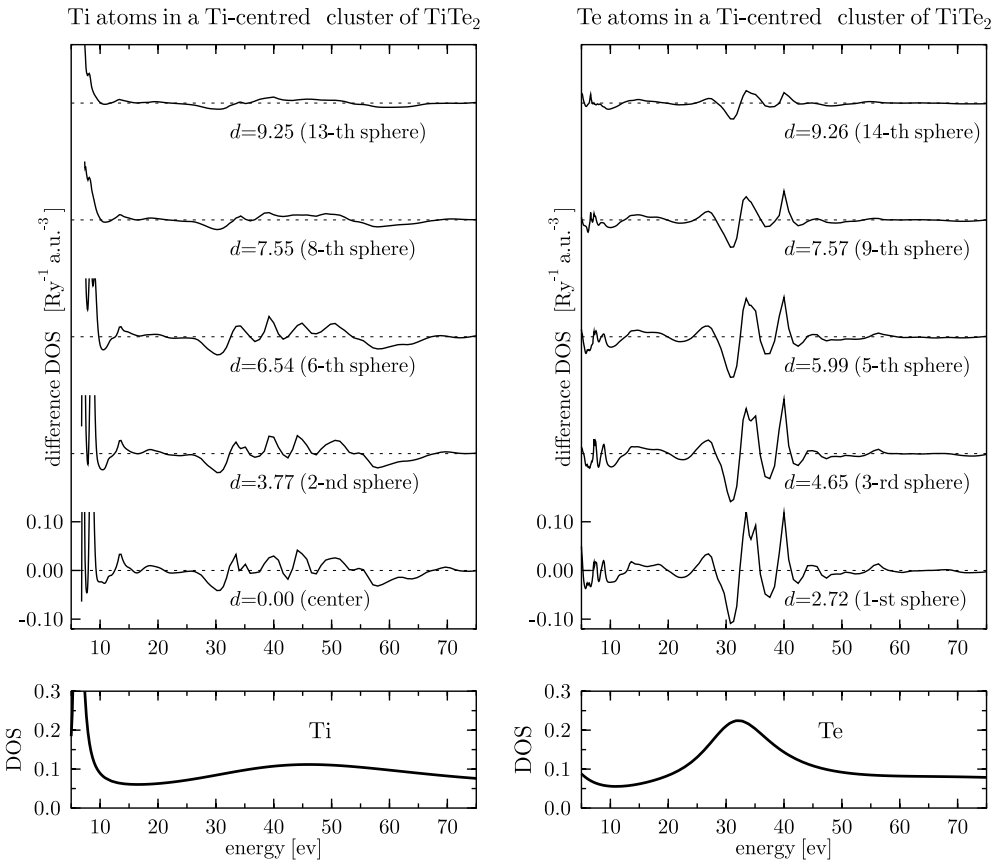

Figure 5. The site-dependent difference density of states $n^{(j)}_{\rm diff}(E)$ around Ti atoms (left panel) and Te atoms (right panel) in a Ti-centred cluster of 135 atoms of $TiTe_2$. Each curve is identified by the order of the corresponding coordination sphere around the central Ti atom and by its distance from the centre in Å. The two lower panels display the total DOS around isolated Ti and Te atoms $n^{(j)}_{\rm at}(E)$. The units are states per Ryd per au^3 in all four panels.

around isolated Ti and Te atoms is shown in the two lower panels and the difference DOS $n_{\mathrm{diff}}^{(j)}(E)$ (cf. equation (6)) is in the upper panels.

The dependence of the difference DOS on the position of the atom in the cluster exhibits similar features to that in the case of bulk copper: the DOS approaches the atomic-like form for those atoms which are sufficiently close to the surface (unlike S atoms in section 4.1).

The atomic DOS is generally larger for tellurium than for titanium (lower panels of figure 5). This is consistent with the generally larger scattering amplitude for tellurium atoms than for titanium ones. However, this fact alone cannot explain different cluster-size convergences for Ti and Te spectra, as the ratio between the numbers of Ti and Te atoms remains approximately equal for the 'critical' sizes of test clusters mentioned at the beginning of this section. Unlike in the case of ZnS, the crystal structure of $TiTe_2$ does not offer any suitable 'focusing candidates'. Hence, we conclude that a purely DOS-oriented viewpoint does not suffice to explain intuitively the cluster-size-effect asymmetry of the XANES of $TiTe_2$. Rather, is has to be a consequence of a complicated interference of many multiple-scattering paths.

5. Conclusions

We found that the local density of unoccupied states around atoms at the surface of a cluster differs from the DOS around bulk atoms mainly owing to the much lower heights of DOS peaks in the former case. For atoms asymmetrically located far away from the centre of a cluster, the DOS around them is more influenced by the presence of even quite distant bulk-like atoms inside the rest of the cluster than by the proximity of the surface itself. Practically all of the fine structure in the excess density of states of electrons around a finite cluster of atoms, determined by the Lloyd formula, arises in the interior of that cluster. The degree of localization of the excess DOS does not depend on the cluster size. The rate at which the DOS around cluster surface atoms approaches the DOS around isolated atoms depends quite a lot on the chemical type of that atom. Analysing the local site-dependent DOS around atoms of different chemical types is a conceptually well-defined and computationally cheap way to gain additional insight into the mechanism of formation of some XANES features. It helps in understanding peculiarities in the cluster-size effect of calculated XANES spectra of some compounds (such as ZnS); however, open questions still remain in other cases (as for $TiTe_2$).

Acknowledgments

This work was supported by the project 202/99/0404 of the Grant Agency of the Czech Republic. The author is grateful to A Šimůnek for stimulating discussions and for a critical reading of the manuscript.

References

[1] Rehr J J and Albers R C 2000 *Rev. Mod. Phys.* **72** 621
[2] Durham P J 1988 *X-ray Absorption: Principles, Applications, Techniques of EXAFS, SEXAFS and XANES* ed D C Koningsberger and R Prins (New York: Wiley) p 53
[3] Lee P A and Pendry J B 1975 *Phys. Rev.* B **11** 2795
[4] Lloyd P and Smith P V 1972 *Adv. Phys.* **21** 69
[5] Vvedensky D D 1992 *Unoccupied Electron States* ed J C Fuggle and J E Inglesfield (Berlin: Springer) p 139
[6] Müller J E and Wilkins J W 1984 *Phys. Rev.* B **29** 4331
[7] Nesvizhskii A I, Ankudinov A L and Rehr J J 2001 *Phys. Rev.* B **63** 094412
[8] Šipr O 2001 *J. Synchrotron Radiat.* **8** 232
[9] Vvedensky D D, Saldin D K and Pendry J B 1986 *Comput. Phys. Commun.* **40** 421

[10] Natoli C R, Misemer D K, Doniach S and Kutzler F W 1980 *Phys. Rev.* A **22** 1104
[11] Ankudinov A L, Ravel B, Rehr J J and Conradson S D 1998 *Phys. Rev.* B **58** 7565
[12] Györffy B L and Stott M J 1973 *Band Structure Spectroscopy of Metals and Alloys* ed D J Fabian and L M Watson (London: Academic) p 385
[13] Durham P J, Pendry J B and Hodges C H 1982 *Comput. Phys. Commun.* **25** 193
[14] Natoli C R, Benfatto M and Doniach S 1986 *Phys. Rev.* A **34** 4682
[15] Šipr O 1996–1999 *Computer code RSMS* Institute of Physics, AS CR, Praha
[16] Moruzzi V L, Janak J F and Williams A R 1978 *Calculated Electronic Properties of Metals* (New York: Pergamon)
[17] Šipr O 2000 unpublished
[18] Sainctavit Ph, Petiau J, Calas G, Benfatto M and Natoli C R 1987 *J. Physique Coll.* **48** C9 1109
[19] Šipr O, Šimůnek A, Bocharov S, Heumann D and Dräger G 1999 *J. Synchrotron Radiat.* **6** 518
[20] Sainctavit Ph, Petiau J, Benfatto M and Natoli C R 1989 *Physica* B **158** 347
[21] Šipr O, Machek P, Šimůnek A, Vackář J and Horák J 1997 *Phys. Rev.* B **56** 13 151
[22] Bocharov S, Dräger G, Heumann D, Šimůnek A and Šipr O 1998 *Phys. Rev.* B **58** 7668